J. Biochem. 126, 559-565 (1999)

Crystal Structure of Prolyl Aminopeptidase from *Serratia marcescens*[1]

Tadashi Yoshimoto,*,[2] Tsutomu Kabashima,* Kouichirou Uchikawa,* Takahiko Inoue,* Nobutada Tanaka,† Kazuo T. Nakamura,† Masato Tsuru,‡ and Kiyoshi Ito*

**School of Pharmaceutical Sciences, Nagasaki University, 1-14 Bunkyo-machi, Nagasaki 852-8521; †School of Pharmaceutical Sciences, Showa University, 1-5-8 Hatanodai, Shinagawa-ku, Tokyo 142-8555; and ‡Information Science Center, Nagasaki University, 1-14 Bunkyo-machi, Nagasaki 852-8521*

Received May 28, 1999; accepted July 1, 1999

Prolyl aminopeptidase from *Serratia marcescens* specifically catalyzes the removal of N-terminal proline residues from peptides. We have solved its three-dimensional structure at 2.3 Å resolution by the multiple isomorphous replacement method. The enzyme consists of two contiguous domains. The larger domain shows the general topology of the α/β hydrolase fold, with a central eight-stranded β-sheet and six helices. The smaller domain consists of six helices. The catalytic triad (Ser113, His296, and Asp268) is located near the large cavity at the interface between the two domains. Cys271, which is sensitive to SH reagents, is located near the catalytic residues, in spite of the fact that the enzyme is a serine peptidase. The specific residues which make up the hydrophobic pocket line the smaller domain, and the specificity of the exo-type enzyme originates from this smaller domain, which blocks the N-terminal of P1 proline.

Key words: α/β hydrolase, proline iminopeptidase, prolyl aminopeptidase, *Serratia marcescens*, X-ray analysis.

Prolyl aminopeptidase (PAP, proline iminopeptidase; EC 3.4.11.5) catalyzes the removal of N-terminal proline from peptides. Many studies have been performed since the first report of the *Escherichia coli* enzyme by Sarid *et al.* (*1*). Different sources of the PAP have been described, implying its wide distribution in nature. However, this enzyme has been found mainly in bacteria and in some plants, and it is not clear whether it is present in animals or not (*2*). In some bacteria, PAP is a component of the proteolytic system. For example, in *Thermoplasma acidophilum*, a novel proteolytic system, unrelated to the 20S proteasome, which consists of a high molecular mass protease named Tricorn protease and PAP, was reported (*3*).

In addition to its inhibition by *p*-chloromercuribenzoate (PCMB) and heavy metals, and because other reagents such as diisopropyl phosphofluoridate (DFP) have little or no affect on it, PAP has been suggested to be a cysteine peptidase. However, we demonstrated by means of site directed mutagenesis, that a serine and not a cysteine residue is essential for the activities of the *Aeromonas sobria* and *Bacillus coagulans* PAPs (*4*). Several *pap* genes have been cloned and sequenced from *A. sobria* (*5*), *B. coagulans* (*6*), *Flavobacterium meningosepticum* (*7*), *Hafnia alvei* (*8*), *Lactobacillus delbrueckii* subsp. *bulgaricus* (*9*), *Neisseria gonorrhoeae* (*10*), *Xanthomonas campestris* pv. *citri* (*11*), and *Serratia marcescens* (*12*). Alignment of the amino acid sequences and consideration of the enzymatic properties showed that the PAP enzymes could be classified into two groups. One consists of monomers of approximately 30 kDa. They are rather small enzymes with a strict specificity for proline terminals and they cannot act on large peptides. The second group comprises multimeric large enzymes of around 200 kDa, with a broader specificity extending to hydroxyproline terminals. These enzymes also act on longer peptide substrates.

To clarify the structure and catalytic mechanism of the enzyme from *S. marcescens*, we crystallized and clarified the three-dimensional structure of the enzyme at 2.3 Å resolution. Recently, the three-dimensional structure of a similar enzyme from *X. campestris* pv. *citri* was reported (*13*). We compared the structures of the two enzymes in this study.

MATERIALS AND METHODS

Materials—Ethylmercurithiosaricylic acid (EMTS) was purchased from Aldrich. Seleno-DL-methionine and the Kao and Michayluk vitamin solution were from Sigma.

Preparation of SPAP Crystals and Heavy Atom Derivatives—SPAP was purified and crystallized using PEG6000 as a precipitating agent as previously described (*12*). The crystals belong to the tetragonal space group, $P4_12_12$ or $P4_12_12$, contain one molecule per asymmetric unit, and have cell constants of $a=b=65.36$ and $c=169.2$ Å. Three

[1] This work was supported in part by a Grant-in-Aid for Scientific Research from the Ministry of Education, Science, Sports and Culture of Japan. Crystallographic coordinates for the prolyl aminopeptidase have been deposited with the Brookhaven Protein Data Bank as entry 1QTR.

[2] To whom correspondence should be addressed. Phone: +81-95-847-1111, Fax: +81-95-843-2444, E-mail: t-yoshimoto@cc.nagasaki-u.ac.jp

Abbreviations: DFP, diisopropyl phosphofluoridate; PAP, prolyl aminopeptidase; PCMB, *p*-chloromercuribenzoate; POP, prolyl oligopeptidase; Pyr, pyroglutamyl; SPAP; *Serratia marcescens* PAP; XPAP; *Xanthomonas campestris* pv. *citri* PAP.

TABLE I. **Concentrations, soaking time, conditions, and data collection statistics for heavy-atom derivatives.**

Compound	Soaking conditions		Limiting resolution (Å)	No. of collected/ unique reflections	Completeness (%)	R_{merge}[a] (%)	R_{iso}[b] (%)	Phasing power[c]	Site
	Conc. (mM)	Time							
Native			2.3	45,646/14,917	89.1	5.9	–	–	–
EMTS[d]	0.3	4 days	2.7	42,252/9,476	90.9	6.9	14.5	1.5	1
$HgCl_2$	0.1	7 hours	2.6	24,654/10,096	76.5	12.7	15.9	0.5	2
$K_2Pt(NO_2)_4$	5	2 days	2.9	15,362/7,719	64.1	8.5	18.2	0.6	3
SeMet			3.5	37,746/10,015	82.7	7.5	9.2	1.2	4

[a] $R_{merge} = \Sigma_h \Sigma_i |I(h)_i - \langle I(h) \rangle| / \Sigma_h \Sigma_i I(h)_i$, where i represents different observations. [b] $R_{iso} = \Sigma_h |F(\text{deriv}) - F(\text{native})| / \Sigma_h F(\text{native})$. [c] Phasing power = rms($|F_H|/E$), $|F_H|$ = heavy atom structure factor amplitude, and E = rms lack of closure. [d] EMTS = ethyl mercury thiosalicylate.

TABLE II. **Crystal data and refinement statistics for SPAP.**

Space group	$P4_32_12$
Cell constants	
a	65.36 Å
b	65.36 Å
c	169.2 Å
Resolution range	8.0-2.3 Å
No. of reflections ($F > 1.0\sigma$)	14,917
Completeness	89.1%
R-factor	18.9%
Free R-factor[a]	26.7%
No. of water molecules	94
Rms deviations from ideal values	
Bond length	0.009 Å
Bond angles	1.39°

[a] A subset of data (10%) was excluded from the target set for refinement and exclusively used for free R value calculation.

heavy atom derivatives [EMTS, $HgCl_2$, and $K_2Pt(NO_3)_4$] were prepared by soaking.

Preparation of the Selenomethionyl PAP—PAP, in which all of the methionine residues were replaced by selenomethionine, was prepared by transfer of pSPAP-HE (*12*) into methionine auxotrophic strain DL41 (*14*). A single, freshly grown colony of pSPSP-HE/DL41 was picked up from an LB plate, put into the medium, which comprised 2% (v/v) LB and 98% (v/v) LeMaster (defined) medium with 50 mg/liter selenomethionine replacing methionine, and 10 ml/liter vitamin solution, and incubated at 30°C. Selenomethionyl SPAP was purified and crystallized in the same manner as the unsubstituted enzyme (*12*).

Data Collection and Processing—X-ray data collection was performed by the oscillation method at 20°C using a Rigaku R-AXIS IIc area detector with graphite-monochromated Cu Kα radiation, which was generated by a Rigaku RU200 rotating-anode X-ray generator (operated at 42 kV and 92 mA). The best native X-ray data set was collected up to 2.3 Å resolution from a single crystal. The data for heavy-atom derivative crystals were respectively collected up to 2.7 Å resolution in a similar way. Each data set was processed with the program, PROCESS, installed in the R-AXIS IIc system. The statistics for the native and derivative data sets are summarized in Table I.

Structure Determination and Refinement—The structure of SPAP was determined by multiple isomorphous replacement (MIR). Heavy-atom parameters were refined with the program, MLPHARE (*15*). The figure-of-merit for the refined phases was 0.611 for centric reflections to 2.7 Å resolution. The MIR phases at 2.7 Å resolution were improved by means of solvent flattening and histogram-matching algorithms, and extended to 2.3 Å resolution using the program, DM (hereafter called MIRDM phases). In order to prevent the loss of surface information, a value (35%) considerably lower than the experimentally estimated value (53%) was employed as the solvent content parameter for the solvent-flattening procedures. The programs used for calculation are included in the CCP4 package (*16*).

All the model building and correction procedures were carried out on a Silicon Graphics O2 workstation, using the program, TURBO-FRODO (*17*). The model was built into MIR and MIRDM electron density maps. In addition, the positions of selenium atoms can be easily determined through the use of the difference Fourier technique.

Structure refinement was performed using the program, X-PLOR (*18*). To built a model for the exposed loop region where the MIR-DM electron density was rather weak, $2F_o - F_c$ and $F_o - F_c$ maps were calculated, and the model was corrected and expanded with the program, TURBO-FRODO. After several rounds of refinement, peaks above 3.0σ in an $F_o - F_c$ map were picked as water molecules. Water molecules having B-values greater than 60 Å^2 were excluded. Ninety-four water molecules were included per asymmetric unit. A summary of the refinement statistics is shown in Table II. The stereochemistry of the model was verified using the software package, PROCHECK (*19*).

RESULTS

Structure Determination—The structure of SPAP was determined by the multiple isomorphous replacement method and refined to an R-factor of 0.189 at 2.3 Å resolution (Fig. 1). Most residues are included in the current model, but the $2F_o$-F_c electron density map disconnected at N, C termini and surface regions; residues 1-3, 215, and 317. On Ramachandran plotting, it was found that a total of 238 non-glycine and non-proline residues have their ϕ, ψ angles in the most favored region of the Ramachandran plot, and the remaining 22 non-glycine and non-proline residues in the additional allowed region. Only one non-glycine residue, Ser113, is in the generously allowed region.

Molecular Structure—A monomer of SPAP has approximate dimensions of 65 Å × 50 Å × 40 Å and consists of two contiguous domains. The lower domain contains six helices (α_A-α_F) and an eight stranded β sheet (residues 4-140 and 244-316). Since the catalytic triad (Ser113, Asp268, and His286) exists in this domain, it is called the "catalytic domain." The N-terminal segment contains six β-strands and three helices. The C-terminal segment contains two β-strands and three helices. This domain exhibits a characteristic α/β hydrolase fold and contains a central eight stranded β-sheet with all strands except the second one

aligned in a parallel manner. The β-sheet is significantly twisted and the topology of β-strands is $+1$, $+2$, $-1x$, $+2x$, $(+1x)_3$ (*22*).

The upper domain contains six helices (α1-α6), and is hereafter called the "helices domain" (residues 141-243). Between the two domains, there is a large cleft and catalytic residues are located on the large cavity. None of the two cysteine residues present in the sequence of SPAP participates in a disulfide bridge.

Active Site—Based on the results of site-directed mutagenesis and alignment of the amino acid sequence, Ser113, Asp268, and His296 were determined to be the catalytic residues of SPAP. Indeed they are clustered in the center of the SPAP molecule and exhibit the same form as other several serine α/β hydrolases.

The active site is located on the large cavity at the interface between the two domains. The entrance of the cavity is wide and lined by hydrophobic residues (Val208, Phe219, Phe224, and Phe228), hydrophilic residues (Ser52, His54, Ser297, and Asp299), and Gly48, Gly49, and Gly50. The bottom of the cavity is made up of hydrophobic residues (Phe139, Phe236, Trp114, Trp148, and Cys271), and Tyr149, Tyr150, and Tyr235. The catalytic residues lie in the center of the cavity. Catalytic Ser113 and His296 are directly exposed to the bulk solvent.

Ser113 is found in the consensus sequence of all known sequences of PAPs and most of the α/β hydrolases (G-X-S-B-Z; B, bulky; Z, small side chain; X, any amino acid). Ser113 connects βE and αC like the tip of an elbow. This is a typical characteristic of the α/β hydrolase fold (strand-nucleophil-helix) (*23*). The main chain conformation of Ser113 is energetically unfavorable, as for other α/β

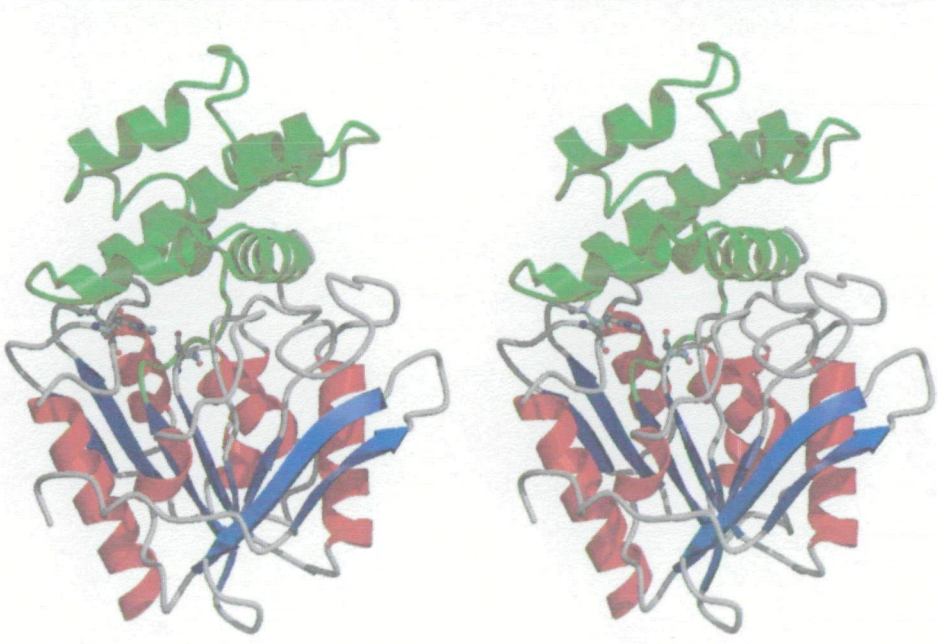

Fig. 1. **Stereo representation of the structure of SPAP.** The three catalytic residues are shown as a ball-and-stick representation. The picture was drawn with MOLSCRIPT (*20*) and rendered with RASTER3D (*21*).

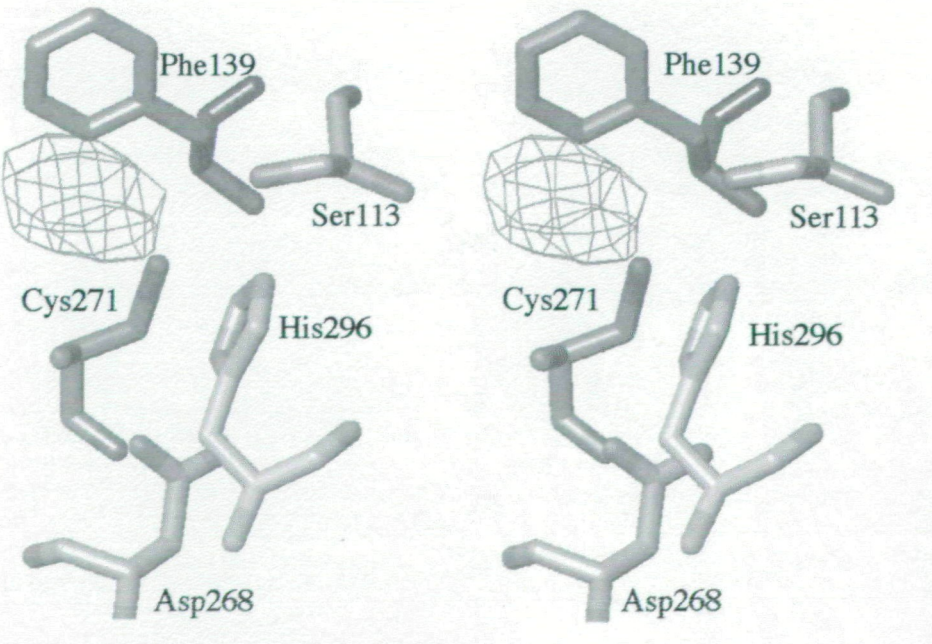

Fig. 2. **$|F_{EMTS}|-|F_{native}|$ electron density map near Cys271.** A stick drawing of Cys271 and its surrounding residues (Ser113, Asp268, His296, and Phe139) is shown. The electron density peak seems to block the specificity pocket.

hydrolases. Furthermore, several small residues (Gly45, Gly46, Gly111, and Gly112) surround Ser113 to prevent steric hindrance.

His296 is located in the middle of the loop situated between βE and αF. The imidazole ring of His296 is situated between Ser113 and Asp268, and suitable for forming the hydrogen bond to each residue, the distance between Ser113 (O^{γ}) and His296 ($N^{\epsilon 2}$) being 2.9 Å and that between His296 ($N^{\delta 1}$) and Asp268 ($O^{\delta 2}$) being 2.7 Å (Fig. 2).

Asp268 is in a position between βG and αE. Among three catalytic residues, only Asp268 is not exposed to water molecules. Similar results have been obtained for the PAP from *X. campestris* pv. *citri* (*14*).

Cysteine Residue—Cys271 is located at the bottom of the cavity, and flanked by the catalytic residues at a distance of 5 Å. At first, PAP was assumed to be a sulfhydryl peptidase, due to its inhibition by PCMB and heavy metals. However, Cys271 is not essential for the activity, but the specificity pocket was blocked by heavy metals. Among heavy atom derivatives, EMTS and $HgCl_2$ were indeed found near Cys271 and seemed to block the S1 pocket (Fig. 2).

Substrate Specificity—The specificity pocket is located on the bottom of the cavity consisting of hydrophobic residues (Ala270, Phe139, Phe236, Trp114, Trp148, and Cys271), Tyr149, Tyr150, and Tyr235, and sized of a Pro residue (Fig. 3).

In the case of serine proteases, two main chain imino protons act as hydrogen bond donors to stabilize the oxyanion intermediate. Consequently, we came to the conclusion that the main chain imino group of highly conserved residues among PAPs, Gly46, and Trp114, shape the "oxyanion hole." Indeed, these two residues are lined by Ser113. Furthermore, Pro47 has an unstable *cis* conformation, and the main chain amino group of Gly46 is arranged so as to protrude toward the P1 carbonyl oxygen (Fig. 4).

In the specificity pocket, Glu204 and Glu232 are stand in a line opposite Ser113 (Fig. 4). They are so close to each other that there might be an electrostatically unfavorable interaction between their charged side chains. However,

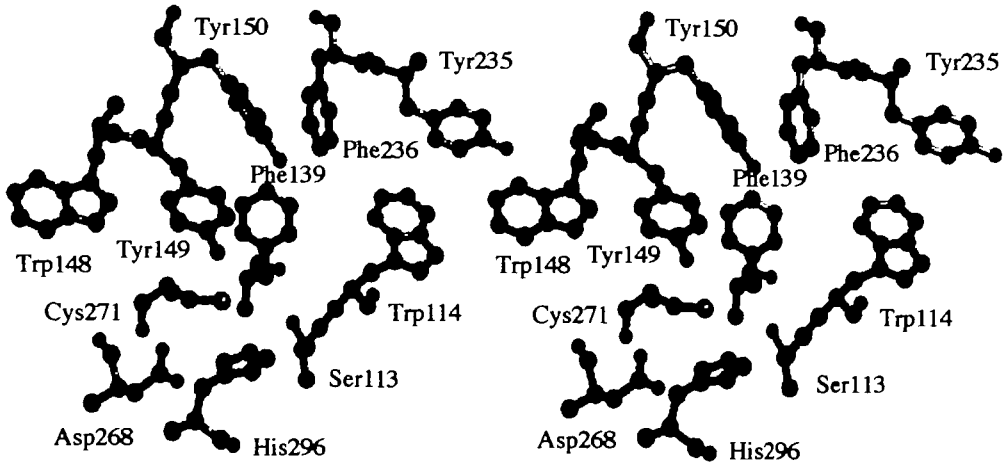

Fig. 3. Stereoview of the specificity pocket around the catalytic triad (Ser113, His-296, and Asp268).

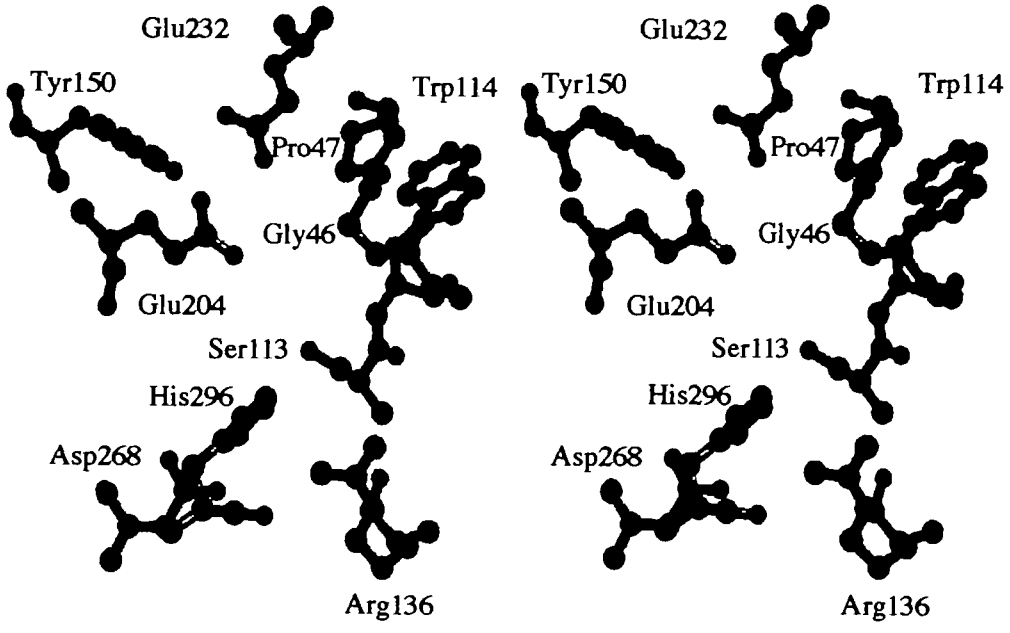

Fig. 4. Stereostick drawing of the specific residues. Glu240 and Glu232 seem to play a role in the binding with the amino terminal group of the substrate. Arg136 is located at the putative S1′ position. Gly46 and Trp114 form the oxyanion hole.

since a water molecule is located near these side chains and they form the hydrogen bonds, the glutamate pair is electrically situated so as to be stabilized. A state of binding substrate, they might play a role in the interaction with the charged amino terminal group of P1 residue.

Another residue that surrounds Ser113 is Arg136 (Fig. 4). The side chain of Arg136 is located in the putative S1′ position, and seems to play a role in the binding to the P1′ carbonyl oxygen.

DISCUSSION

The prolyl oligopeptidase family is characterized by the sequential order of the catalytic triad (Ser, Asp, and His), that is different from those of other serine proteases. This family consists of PAP, prolyl oligopeptidase (prolyl endopeptidase, POP), and dipeptidyl peptidase IV, and specifically cleaves internal Pro-X bonds. We proposed that the enzymes belonging to the prolyl oligopeptidase family contain the α/β hydrolase fold as a common structure (*12, 24*). In this study, we clarified that SPAP indeed has an α/β hydrolase fold. Beside PAP, lipases, esterases, serine carboxypeptidases, and several hydrolases contain an α/β hydrolase fold (*25-28*). This is indicates that these enzymes including the prolyl oligopeptidase family have a common ancestor.

Very recently, PDB data for XPAP became available. Since the amino acid sequence of SPAP exhibits 54% identity to that of XPAP, the overall topologies of the two enzymes are very similar, especially around the catalytic triad (Fig. 5). However, SPAP is a monomer and its crystal contains one molecule per asymmetric unit, while XPAP is a multimer and its crystal contains one dimer per asymmetric unit. The reason for the difference is not clear, but the sequence concerning the intersubunit contact of XPAP exhibits lower identity (32%) with the corresponding sequence of SPAP than the overall identity, suggesting that the monomer-monomer interaction binding on the surface of SPAP and XPAP is different.

SPAP consists of two contiguous domains, the "catalytic" and "helices" domains, like XPAP. Between the two domains, there is a large cleft and catalytic residues are located on the large cavity. The putative S1 pocket, according with the bottom of the cavity, consists of hydrophobic residues and several tyrosines, forming a hydrophobic pocket. This pocket is a suitable size for proline, and it seems to be fixed through the hydrophobic interaction. The crystal structure of POP was solved by Fülöp *et al.* (*29*). The substrate binding pocket was mapped based on the complex formed between the enzyme and the specific inhibitor, Z-Pro-prolinal. The S1 specificity pocket ensures a hydrophobic environment and a snug fit for the proline residue. Recently, we solved the crystal structure of pyroglutamyl peptidase I (PGP; EC 3.4.11.8) (*30*). PGP is able to specifically remove the amino terminal pyroglutamyl (Pyr) residue, which is structurally analogous to proline. At the active site of PGP, catalytic residues are also located on the pocket consisting of hydrophobic residues. The three-dimensional structure of another proline specific enzyme, aminopeptidase P, which cleaves X-Pro bonds, has been clarified (*31*). However, the enzyme is a metalloenzyme and the three-dimensional data are not available yet. Therefore, the recognition mechanism of aminopeptidase P as to proline is not clear. Accordingly, a hydrophobic interaction and a space suitable for proline in the hydrophobic pocket might be essential for the proline specificity.

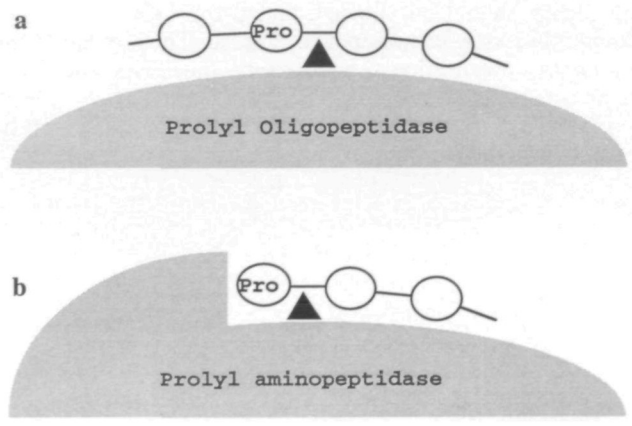

Fig. 6. Illustration of the structural elements of POP (a) and PAP (b).

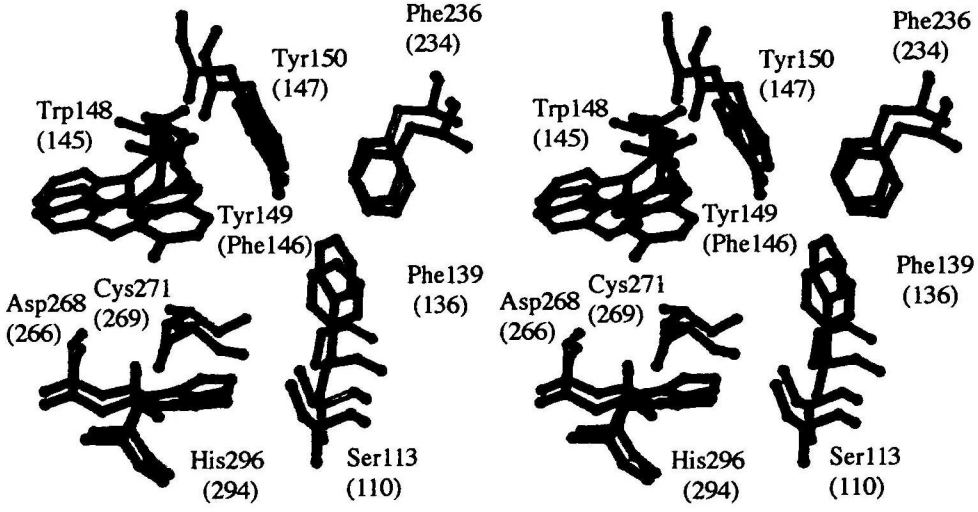

Fig. 5. Comparison of the active sites of SPAP (black) and XPAP (white). The numbers in parentheses are for XPAP.

Since PAP was inhibited by PCMB but not by DFP, the enzyme was first identified as a cystein enzyme (*32*). As shown in Fig. 2, on $|F_{EMTS}|-|F_{native}|$ electron density mapping Cys271 was found to be located near the catalytic triad heavy metal bound to the cystein residue blocking the S1 pocket. A PCMB-sensitive cystein residue was seen as a neighbor of the catalytic triad or S1 pocket in prolyl oligopeptidase (*29*) and carboxypeptidase Y (*33*), which belong to the α/β hydrolase fold superfamily, while the role of the cystein residue in the enzyme is not clear.

PAP catalyzes the removal of an N-terminal proline from peptides (exopeptidase), while POP cleaves peptide bonds on the carboxyl sides of proline within peptides (endopeptidase). As shown in Fig. 6, the mechanism of exopeptidase on PAP has been estimated the presence of the wall. The wall consists of Tyr149, Tyr150 come from α1, and Phe236 from α5 occupy the supposed P2 position of the helices domain (Fig. 3). POP also consists of two domains, one forms the α/β hydrolase fold and exhibits topologically significant similarity to the catalytic domain of SPAP. This domain is defined as the catalytic domain. It is indicated that the catalytic mechanisms of PAP and POP should be consistent or very similar. The other domain forms "β-propellers," which are based on a 7-fold repeat of four-stranded antiparallel β-sheets. The sheets are twisted and radially arranged around their central tunnel. The endo-type specificity should be allowed due to the lack of a helices domain blocking P2 amino acid (Fig. 6). Thus, many of the elements determining the substrate specificity and functions come from the helices domain.

In conclusion, SPAP consists of two domains, catalytic and helices domains. The catalytic domain forms the α/β hydrolase fold. The specificity toward P1 proline should be determined by the hydrophobic residues which make up the hydrophobic pocket. The other specific residues are the glutamate pair (Glu204 and Glu232) and Arg136 (Fig. 7). The specific residues which make up the hydrophobic pocket are lined up in the helices domain. Furthermore, the exo-type specificity might be explained by the helices domain which blocks the N-terminal of P1 proline.

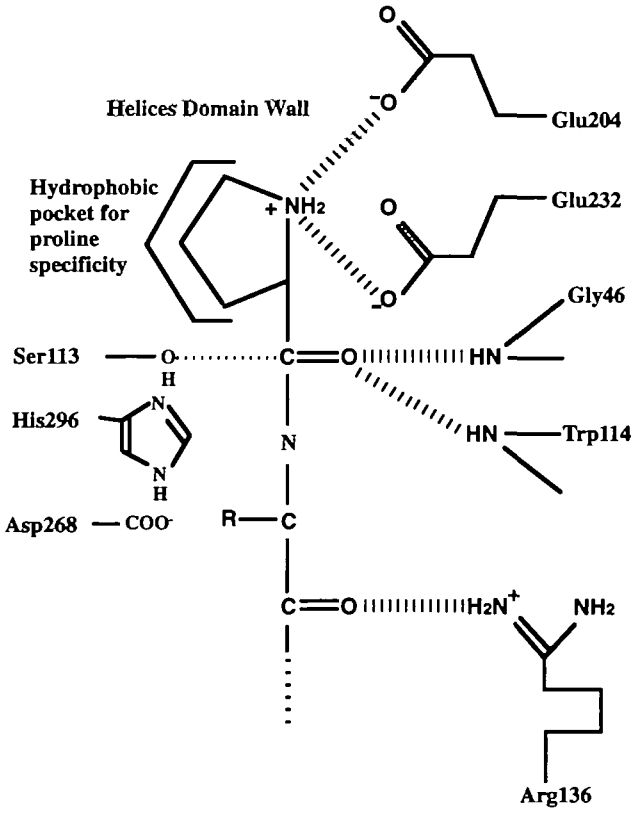

Fig. 7. **Scheme of the active site of SPAP.**

We wish to thank Prof. Y. Mitsui, Dr. T. Nonaka, and Dr. T. Senda (Nagaoka University of Technology) for the advice concerning the method for the selenomethionyl enzyme.

REFERENCES

1. Sarid, S., Berger, A., and Katchalski, E. (1959) Proline iminopeptidase. *J. Biol. Chem.* **234**, 1740–1744
2. Turzynski, A. and Mentlein, R. (1990) Prolyl aminopeptidase from rat brain and kidney: Action on peptides and identification as leucyl aminopeptidase. *Eur. J. Biochem.* **190**, 509–515
3. Tamura, T., Tamura, N., Lottspeich, F., and Baumeister, W. (1996) Tricorn protease (TRI) interacting factor 1 from *Thermoplasma acidophilum* is a proline iminopeptidase. *FEBS Lett.* **359**, 173–178
4. Kitazono, A., Ito, K., and Yoshimoto, T. (1994) Prolyl aminopeptidase is not a sulfhydryl enzyme: Identification of the active serine residue by site-directed mutagenesis. *J. Biochem.* **116**, 943–945
5. Kitazono, A., Kitano, A., Tsuru, D., and Yoshimoto, T. (1994) Isolation and characterization of the prolyl aminopeptidase gene (*pap*) from *Aeromonas sobria*. Comparison with the *Bacillus coagulans* enzyme. *J. Biochem.* **116**, 818–825
6. Kitazono, A., Yoshimoto, T., and Tsuru, D. (1992) Cloning, sequencing, and high expression of the proline iminopeptidase gene from *Bacillus coagulans*. *J. Bacteriol.* **174**, 7919–7925
7. Kitazono, A., Kabashima, T., Huang, H.-S., Ito, K., and Yoshimoto, T. (1996) Prolyl aminopeptidase gene from *Flavobacterium meningosepticum*: Cloning, purification of the expressed enzyme, and analysis of its sequence. *Arch. Biochem. Biophys.* **336**, 35–41
8. Kitazono, A., Kabashima, T., Ito, K., and Yoshimoto, T. (1996) Prolyl aminopeptidase is also present in *Enterobacteriaceae*: Cloning and sequencing of the *Hafnia alvei* enzyme gene and characterization of the expressed enzyme. *J. Biochem.* **119**, 468–474
9. Atlan, D., Gilbert, C., Blanc, B., and Portalier, R. (1994) Cloning sequencing and characterization of the *pepIP* gene encoding a proline iminopeptidase from *Lactobacillus delbrueckii* subsp. *bulgaricus* CNRZ397. *Microbiology* **140**, 527–535
10. Albertson, N. and Koomey, M. (1993) Molecular cloning and characterization of a proline iminopeptidase gene from *Neisseria gonorrhoeae*. *Mol. Microbiol.* **9**, 1203–1211
11. Alonso, J. and Garcia, J.L. (1996) Proline iminopeptidase gene from *Xanthomonas campestris* pv. *citri*. *Microbiology* **142**, 2951–2957
12. Kabashima, T., Kitazono, A., Kitano, A., Ito, K., and Yoshimoto, T. (1997) Prolyl aminopeptidase from *Serratia marcescens*: Cloning of the enzyme gene and crystallization of the expressed enzyme. *J. Biochem.* **122**, 601–605
13. Medrano, F.J., Alonso, J., Garcia, J.L., Romero, A., Bode, W., and Gomis-Rüth, F.X. (1998) Structure of proline iminopeptidase from *Xanthomonas campestris* pv. *citri*: a prototype for the prolyl oligopeptidase family. *EMBO J.* **17**, 1–9
14. Hendrickson, W.A., Horton, J.R., and LeMaster, D.M. (1990) Selenomethionyl proteins produced for analysis by multiwavelength anomalous diffraction (MAD): a vehicle for direct determination of three-dimensional structure. *EMBO J.* **5**, 1665–1672
15. Otwinowski, Z. (1991) Maximum likelihood refinement of heavy atom parameters In *Isomorphous Replacement and Anomalous Scattering* (Wolf, W., Evans, P.R., and Leslie, A.G.W., eds.) pp.

80-86, Daresbury Laboratory, Warrington, England
16. Collaborative Computational Project, Number 4 (1994) The CCP4 suit: programs for protein crystallography. *Acta Cryst.* **D50**, 760-763
17. Roussel, A. and Cambilleau, C. (1992) TURBO-FRODO, Biographics, LCCMB, Marseille, France
18. Brünger, A.T. (19892) *X-PLOR Version 3.1: A System for Crystallography and NMR*, Yale University Press, New Haven
19. Laskowski, R.A., McArthur, M.W., Moss, D.S., and Thornton, J. (1993) PROCHECK: a program to check the quality of protein structures. *J. Appl. Crystallogr.* **26**, 282-291
20. Kraulis, P.J. (1991) MOLSCRIPT: a program to produce both detailed and schematic plots of protein structures. *J. Appl. Cryst.* **24**, 946-950
21. Merritt, E.A. and Murphy, M.E.P. (1994) Raster3D Version 2.0 —A program for photorealistic molecular graphics. *Acta Cryst.* **D50**, 869-873
22. Richardson, J.S. (1981) The anatomy and taxonomy of protein structure. *Adv. Protein Chem.* **34**, 167-339
23. Ollis D.L., Cheah, E., Cygler, M., Dijkstra, B., Frolow, F., Franken, S.M., Harel, M., Remington, S.J., Silman, I., Schrag, J., Sussman, J.L., Verschueren, K.H.G., and Goldman, A. (1992) The α/β hydrolase fold. *Protein Eng.* **5**, 197-211
24. Kabashima, T., Fujii, M., Meng, Y., Ito, K., and Yoshimoto, T. (1998) Prolyl endopeptidase from *Sphingomonas capsulata*: Isolation and characterization of the enzyme and nucleotide sequence of the gene. *Arch. Biochem. Biophys.* **358**, 141-148
25. Schrag, J.D., Li, Y., Wu, S., and Cygler, M. (1991) Ser-His-Glu triad forms the catalytic site of the lipase from *Geotrichum candidum*. *Nature* **351**, 761-764
26. Sussman, J.L., Harel, M., Frolov, F., Oefner, C., Goldman, A., Toker, L., and Silman, I. (1991) Atomic structure of acetylcholinesterase from *Torpedo californica*: A prototypic acetylcholine-binding protein. *Science* **253**, 872-879
27. Endrizzi, J.A., Breddam, K., and Remingtonm S.J. (1994) 2.8 Å structure of yeast serine carboxypeptidase. *Biochemistry* **33**, 11106-11120
28. Pathak, D. and Ollis, D. (1990) Refined structure of dienelactone hydrolase at 1.8 Å. *J. Mol. Biol.* **214**, 497-525
29. Fülöp, V., Böcskei, Z., and Polgár, L. (1998) Prolyl oligopeptidase: An unusual β-propeller domain regulates proteolysis. *Cell* **94**, 161-170
30. Odagaki, Y., Hayashi, A., Okada, K., Hirotsu, K., Kabashima, T., Ito, K., Yoshimoto, T., Tsuru, D., Sato, M., and Clardy, J. (1999) The crystal structure of pyroglutamyl peptidase I from *Bacillus amyloliquefaciens* reveals a new structure for a cysteine protease. *Structure* **7**, 399-411
31. Wilce, M.C.J., Bond, C.S., Dixon, N.E., Freeman, H.C., Guss, J.M., Lilley, P.E., and Wilce, J.A. (1998) Structure and mechanism of a proline-specific aminopeptidase from *Escherichia coli*. *Proc. Natl. Acad. Sci. USA* **95**, 3472-3477
32. Yoshimoto, T. and Tsuru, D. (1985) Proline iminopeptidase from *Bacillus coagulans*: Purification and enzymatic properties. *J. Biochem.* **97**, 1477-1485
33. Endrizzi, J.A., Breddam, K., and Remington, S.J. (1994) 2.8 Å structure of yeast serine carboxypeptidase. *Biochemistry* **33**, 11106-11120